Studying Surface Glass-to-Rubber Transition Using Atomic Force Microscopic Adhesion Measurements

O. K. C. Tsui,* X. P. Wang, Jacob Y. L. Ho, T. K. Ng, and Xudong Xiao

Department of Physics, Hong Kong University of Science and Technology, Clear Water Bay, Kowloon, Hong Kong, China

Received August 30, 1999; Revised Manuscript Received February 22, 2000

ABSTRACT: Force−distance curves were obtained using a home-built atomic force microscope (AFM) at different temperatures (T = 30−65 °C) and probe rates (f = 31.25−50 000 Hz) on a 150 nm thick film of a model sample, poly(*tert*-butyl acrylate) (M_w = 148K Da, M_w/M_n = 17, and T_g^{bulk} = 50 °C according to DSC). The pull-off force, F_{ad}, at which detachment between the AFM tip and the sample occurred was measured as adhesion. By limiting the loading force, F, to ∼2.5 nN, the tip penetrated by no more than 2 nm into the sample in the glassy state. Therefore, evolution of the rheological properties of the polymer at the free surface with increasing T could be studied. In the vicinity of T_g^{bulk}, F_{ad} was seen to increase rapidly with increasing T or decreasing f. Equivalence between T and f was found using time−temperature superposition in which, upon rescale of f by a temperature-dependent shift factor $a_T^{AFM}(T)$, a master curve $F_{ad}(a_T^{AFM}(T)\, f)$ resulted. We showed that $F_{ad}(a_T^{AFM}(T)f)$ could be fully accounted for by using an approach based on fracture mechanics of viscoelastic solids. No noticeable enhancement in the surface relaxation could be deduced according to our findings.

Introduction

Molecular structure and segmental mobility of a polymer within a few nanometers of the surface has significant influence on its application as adhesives, lubricants, biosensors, and protective coatings. In crystalline solids, as a result of the reduced number of bond pairs per atom at a surface, either "reconstruction" or "relaxation" of atomic arrangements in the top layers occurs to lower the surface free energy.[1] Similarly in polymers, the molecular structure and thermodynamics at the surface differs from that of the bulk, leading to notably different phase behaviors near the surface.[2−7]

Of considerable debate recently is the surface mobility of polymers. Computer simulations on polymer chains in a melt near an impenetrable wall indicated an enrichment of chain ends within two polymer segment lengths of the interface.[3] On the basis of entropy considerations, Mayes[4] argued that the chain end groups would preferentially segregate to the polymer/air interface. Since there is more free volume associated with chain ends, this will render the T_g at the surface lower than the bulk. Experimental evidence of chain end segregation to the surface had been found in dynamic secondary ion mass spectroscopy (DSIMS) measurements of Kajijama et al.[6] and neutron reflectivity measurements of Zhao et al.[7] on end-labeled polystyrene (PS) samples. As a result, an important question has yet to be answered, namely, whether enrichment in chain ends will result in observably higher chain mobility and/or reduced T_g at the free surface of polymeric materials. Conclusions from previous studies remain controversial. Using near-edge X-ray absorption fine structure (NEXAFS), Liu et al.[8] studied the relaxation of a small deformation imposed on the free surface of a polystyrene sample. Data monitored for the first 10 and 100 Å of the surface indicated no evidence for enhanced mobility. By studying the lifetime of low-energy positronium implanted in polystyrene, Xie et al.[9] found that the T_g at ∼ 40 Å from the free surface of the polymer was the same as the T_g of the bulk. On the other hand, scanning force microscopy measurements of Kajiyama et al.[10,11] revealed that the surface of polystyrene films was already in a viscoelastic state even at room temperature, if the number-average molecular weight, M_n, of the polymer was less than ∼30K Da. On the basis of temperature-dependent X-ray photoelectron spectroscopic (TDXPS) and angle-dependent XPS (ADXPS) measurements on poly(styrene-*block*-methyl methacrylate), Kajiyama et al.[12] concluded that the T_g of the polymer got progressively smaller than that of the bulk toward the free surface. Using temperature-equivalent time scales, Hammerschmidt et al.[13] produced friction master curves for the data they obtained from temperature-controlled friction force microscopy (FFM) and concluded that the measured T_g's of poly(methyl methacrylate) (PMMA), polystyrene (PS), and poly(ethylene terephthalate) were lower than the respective values of the bulk.

An interesting consequence connected with the existence of a surface mobile layer is the depression in the T_g recently observed by many researchers in confined polymer systems as the size of confinement is decreased.[13−18] (Although the opposite behavior has also been found, it is generally believed to be due to the attractive interactions between the polymer segments and the confining wall, which is not related to the present investigation of the free surface of the polymer.[19]) In the case of polymer thin films, Keddie et al.[14] postulated a mechanism in which a thin surface rubbery layer, existing well below the bulk T_g, thickened as T was increased. The glass transition of a thin polymer film would thus be reached when the thickness of this surface rubbery layer, $\xi(T)$, became equal to the thickness of the film, d. These authors found that the empirical form $\xi(T) = \xi(0)(1 - T_g(d)/T_g^{bulk})^{-\mu}$ fit their data very well, with $\xi(0) \sim 10$ nm and $\mu \sim 0.5$ for the systems they had studied, namely, PS spin-coated on silicon with a native oxide layer and PMMA on gold.

* To whom correspondence should be addressed. E-mail: phtsui@ust.hk.

10.1021/ma991473x CCC: $19.00
Published on Web 04/30/2000

In this paper, a home-built AFM was used to measure the force−distance curves of a 150 nm thick film of poly(*tert*-butyl acrylate) (P*t*BuA) (M_w = 148K Da, M_w/M_n = 17) at different temperatures (T = 30−65 °C) and probe rates (f = 31.25−50 000 Hz; the definition is given in the Experimental Section). The maximum loading force, F, was controlled to ∼2.5 nN so that the AFM tip penetrated no more than 2 nm of the sample surface (see below for the estimate) in the glassy state of the polymer. One would thus expect any thickening of a surface rubbery layer with increasing T that began well below T_g^{bulk} should lead to a noticeably early onset of viscoelastic behavior detectable by the present protocol. From the force−distance curves, we determined the adhesive force, F_{ad}, between the sample and the AFM tip. Glass-to-rubber transition was related to the probe rate and/or temperature dependence of F_{ad}. Correlation between adhesive bond strength and glass-to-rubber transition is indeed well documented in the literature. In studies of fracturing of adhesive bonds,[20−22] master curves were obtained from plots of adhesive bond strength versus peeling rate upon rescaling the abscissa by the WLF shift factor.[23] In the present study, a similar master curve was also obtained for F_{ad}, in which the adhesive force was found to increase as the rescaled frequency (= $a_T^{AFM}(T)f$, where $a_T^{AFM}(T)$ is the shift factor determined from the AFM data) was below ∼10^4 Hz and saturated when it is ∼100 Hz at an arbitrarily chosen reference temperature, T_{ref} = 55 °C. (By definition, the shift factor equals one at $T = T_{ref}$.) The saturation thus seen could be associated with the onset of mechanical yield of the polymer as evidenced by the appearance of a plastic deformation tail in the corresponding force−distance curves. We found that $a_T^{AFM}(T)$ reproduced the shift factor determined from torsion modulus and shear modulus data of the bulk sample. Using fracture mechanics of viscoelastic solids, we showed theoretically that adhesion was directly related to the sample's dynamical compliance, $J(t)$ under the present experimental conditions, which interpretation accounted for the AFM data very well. On the basis of these results, no enhanced molecular relaxation is found at the free surface of the polymer.

Experimental Section

Samples. Poly(*tert*-butyl acrylate) (P*t*BuA) was purchased from Scientific Polymer Products, Inc., Ontario, NY, and was used without further purification. The molecular weight of the polymer was determined by a Waters gel permeation chromatograph (GPC) system. Degassed tetrahydrofuran was used as the eluent at a flow rate of 1.0 mL/min. The working wavelength of the UV detector in the GPC system was set at 254 nm. The molecular weight distribution obtained has M_w = 148K Da and M_w/M_n = 17. The bulk T_g of the polymer was estimated to be 50 °C by a Setaram DSC 92 system at a heating rate of 10 °C/min in dry N_2. This sample has been chosen in the present study as a model sample to demonstrate the technique due to its T_g value being intermediate in the temperature range of operation of our AFM (room temperature to ∼80 °C). Viscoelastic properties of the bulk sample was characterized by measuring the dynamic torsion modulus, $G_{torsion}(\omega/2\pi)$, from T = 60 to 90 °C and the dynamic shear modulus, $G_{shear}(\omega/2\pi)$, from T = 25 to 60 °C, with the oscillatory frequency of the applied torque, $\omega/2\pi$, being varied from 0.016 to 16 Hz (Rheometrics RMS-800, Piscataway, NJ, in parallel plate geometry and torsion rectangular geometry, respectively.) The WLF shift factor for the bulk polymer, $a_T^{bulk}(T)$, could therefore be derived from these data. The master curves for the real part of the resultant dynamic moduli as a function of the rescaled frequency, $a_T^{bulk}\omega/2\pi$, at T_{ref} = 55 °C are shown in the upper panel of Figure 1, and those for the loss tangents are shown in the lower panel. Two dynamic transitions, signified by peaks in the loss tangents (notably one at $a_T^{bulk}\omega/2\pi \sim 0.5$ Hz and the other one emerging at $a_T^{bulk}\omega/2\pi < 10^{-6}$ Hz), are apparent, whose origin can be traced to the glass-to-rubber transition and the flow transition, respectively. Thin films of P*t*BuA (∼150 nm thick according to variable-angle spectroscopic ellipsometry) were prepared by spin-coating 3% solution of the polymer in toluene at 500 rpm. The root-mean-square surface roughness was estimated to be ∼0.9 nm from 0.5 × 0.5 μm^2 AFM topographical scans of the sample. Prior to the initial study, samples were annealed in a vacuum oven at 120 °C overnight and kept inside a dehumidifying box when not in use. Good reproducibility of the AFM data taken 2 months apart indicates high stability of the sample surface.

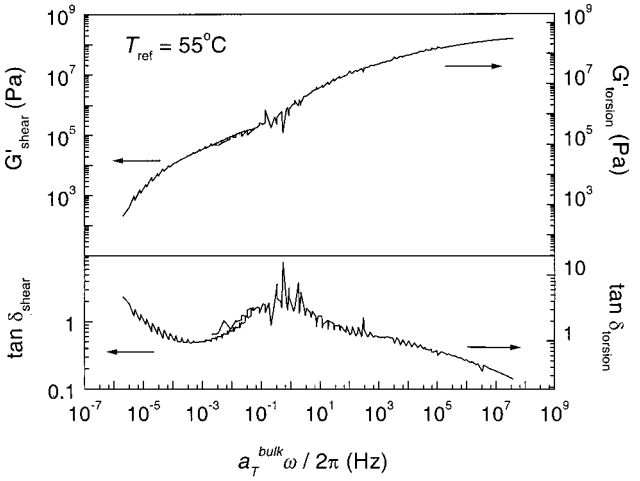

Figure 1. (upper panel) Master curve for the real part of the shear modulus and that of the torsion modulus of poly(*tert*-butyl acrylate) as a function of the rescaled oscillatory frequency of the applied torque, $a_T^{bulk}\omega/2\pi$, in log−log scales. The reference temperature, T_{ref}, has been arbitrarily chosen to be 55 °C. (lower panel) Corresponding data for the loss tangents.

Technique. Force−distance curves and adhesion data presented in this paper were obtained by a home-built AFM controlled by RHK electronics (RHK Technology, MI). Temperature was controlled manually to ±1 °C with a dc current applied through a Peltier heater. Commercial V-shaped silicon nitride integrated tip/cantilevers (Parks Scientific Instruments, Sunnyvale, CA) with nominal force constant $k_c \sim 0.5$ N m^{-1} and radius of curvature of the pyramidal tip $R \sim 50$ nm were used. Measurements were carried out inside a glovebox where the humidity was kept below 10%. Vertical displacement of the cantilever, δ_{piezo}, was adjustable to within 0.02 nm resolution via the voltage applied to the piezoelectric tubes to which the cantilever was attached. Figure 2a shows a typical force−distance curve obtained with our setup. The horizontal axis represents δ_{piezo} and the vertical axis the applied load, $F = k_c\delta_{tip}$, where δ_{tip} is the deflection of the cantilever (see Figure 2b for illustration.) In practice, δ_{tip} is monitored by the deflection of a laser beam reflected from the top surface of the tip using a quadrant photodetector. By using a hard sample for which δ_{tip} always equals δ_{piezo}, the photodetector reading can be calibrated to give δ_{tip}. The pull-off force that causes detachment between the sample and the tip is measured as adhesion, F_{ad}. To reduce statistical noise, each datum of F_{ad} was determined by averaging from 10 to 30 independent measurements. A ±10% variation in F_{ad} determined with different tips was however still found, which is probably due to the variance in k_c and R of the commercial product. For convenience, in cases where the force−distance curves do not exhibit a sharp snap-out of the tip at detachment, but rather a plastic deformation tail persists, F_{ad} is determined as the maximum pull-off force recorded in the force−distance curve. During the operation, advancement or withdrawal of

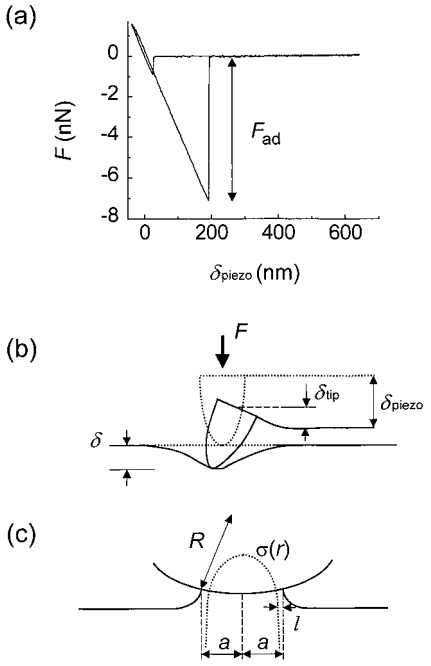

Figure 2. (a) Typical force−distance curve obtained from our setup, in which derivation of adhesion, F_{ad}, is also indicated. (b) Schematic diagram exemplifying the relation between the displacement of the cantilever, δ_{piezo}, bending of the cantilever tip, δ_{tip}, and indentation of the polymer, δ. (c) Schematic diagram showing the radius of the contact between the polymer and the tip, a, the stress distribution, $\sigma(r)$ (dotted line), and the crack length, l.

the cantilever was taken in steps of 0.16 nm over a preset time interval δt adjustable from 4 μs to 640 ms. In physical terms, δt is the time over which the applied load stays constant at any given value before a stepwise change (that will give rise to a change of 0.16 nm in the cantilever displacement) is imposed. Therefore, any dynamical property being probed is expected to reflect the response of the polymer at a delay time $\sim \delta t$. We define the probe rate, f, as $1/\delta t$.

Theory. It is important to understand on theoretical grounds how the present approach may detect the presence of a thermally expanding rubbery layer at the free surface of a polymer, which is one purpose of this study. The sample indentation, δ, is related to δ_{tip} and δ_{piezo} by

$$\delta_{piezo} = \delta_{tip} + \delta = \delta_{tip}(1+ k_c/k_s) \quad (1)$$

where $k_s = dF/d\delta$ is the effective force constant of the sample. Here, use has been made from the fact that the Young modulus of P*t*BuA (≤0.6 GPa in this study) is much smaller than that of silicon nitride (∼155 GPa[25]); negligible deformation can therefore be assumed for the tip. Contact mechanics between two spherical objects under the action of an interfacial surface energy, γ, has been studied by Johnson, Kendall, and Roberts (JKR).[24] Modified to suit our experimental conditions, the model leads to

$$a^3 = \frac{3(1-\nu^2)R}{4E}[F + 3\gamma\pi R + \sqrt{6\gamma\pi RF + (3\gamma\pi R)^2}] \quad (2)$$

$$F_{ad} = -\frac{3}{2}\pi\gamma R \quad (3)$$

$$a_{detach}{}^3 = \frac{9}{8}\pi\gamma(1-\nu^2)\frac{R^2}{E} \quad (4)$$

where a is the contact radius between the polymer and the tip (see Figure 2c), ν is the Poisson ratio and E the Young modulus of the polymer, and a_{detach} is the value of a just before detachment. When the polymer is glassy, $E \sim 0.6$ GPa and $\gamma \sim 24$ erg cm^{-2} (based on the experimentally measured F_{ad}.) If F is controlled to ∼2.5 nN and ν assumes the value 0.5, one will have $a \sim 12$ nm, $\delta \sim 1.2$ nm, and $a_{detach} \sim 6.4$ nm. However, when the polymer becomes rubbery and softens to make $E \sim 10$ MPa, we note a 5-fold increase in γ (which is related to the increase in the dynamic compliance of the polymer and will be discussed later), so we obtain $a \sim 63$ nm ($>R$) and $a_{detach} \sim 40$ nm, which estimate for a obviously invalidates the model's presumption that the tip is spherical. One will simply expect the tip to penetrate a distance comparable to R into the polymer. However, inappropriateness of the JKR model in cases as such to predict the mechanics at loading should not preclude its applicability to conditions at detachment, if the anticipated value of a_{detach} is less than R. As the JKR results are solutions to the equilibrium states, the contact radius and applied force at loading should not bear any relevance to the contact radius and pull-off force at unloading, as is evident in eqs 3 and 4. In particular, the value of a_{detach} is set by the condition when a, expressed in eq 2, just becomes imaginary during pull-off (where $F < 0$), which also turns out to be the minimum value a attains. Independence of a_{detach} (and F_{ad}) on the loading history leads to interesting consequences. Imagine now that we have a very thin layer of softened polymer coated on a hard substrate. Further assume that the thickness of the softened polymer is less than $R - \sqrt{(R^2 - a_{detach}{}^2)}$, where a_{detach} is the contact radius at detachment predicted by eq 4 for the softened polymer. Being obstructed by the hard substrate underneath, protrusion of the tip will terminate at an initial contact radius that is smaller than a_{detach}. The JKR model will obviously break down in this case, as a_{detach} is the minimum contact radius two *homogeneous* objects in contact may acquire. The resultant mechanical problem complicates into one that involves a tip and a composite consisting of the rubbery layer and the substrate. Adhesion is probably going to be intermediate between that for the softened polymer and that for the hard substrate. The foregoing discussion warrants the following scenario: Assume that the dynamic inhomogeneity proposed by Keddie et al. prevails. At very low temperatures when the thickness of the surface rubbery layer is so small that the contact radius is less than a_{detach}, it will be penetrated by the tip right through into the underlying glassy region. Because of the discussions above, F_{ad} will be smaller than the value expected for the rubbery layer. As temperature is increased and reaches the point where the surface rubbery layer is thick enough that the contact radius becomes bigger than the value of a_{detach} expected for the rubbery layer, the full strength of F_{ad} for the rubbery state will recover. Assuming the parameters used above for a softened polymer with $E \sim 10$ MPa, this will happen when the rubbery layer becomes 9 nm thick. Studies on thin P*t*BuA films conform to our interpretation, wherein increase in F_{ad} with increasing T happens only when the film thickness is more than ∼ 9 nm. Therefore, the onset of viscoelastic behavior at a given probe rate is expected to occur at a temperature much below that for the bulk if an expanding surface rubbery layer did exist.

Results

Temperature Dependence. Figure 3 shows the data for F_{ad} vs T obtained at a fixed probe rate of 125 Hz and incremental temperatures from 30 to 65 °C with 30 min being allowed at each temperature for thermal equilibration. As seen, F_{ad} increases gradually from 5.7 nN at $T = 30$ °C to 29 nN at $T = 65$ °C. No noticeable difference in the result could be observed when the measurement was repeated at cooling. Similar studies on a bare silicon substrate showed no temperature dependence in the measured adhesion, indicating that any parameters in the setup that change with temperature such as k_c will not affect our adhesion measurement over the temperature range studied. To see the relation between changes in adhesion and changes in

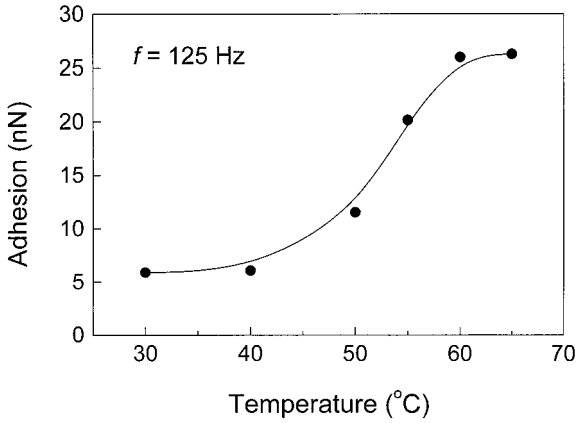

Figure 3. Adhesion vs temperature obtained at a probe rate of 125 Hz. Solid line is a guide to the eye.

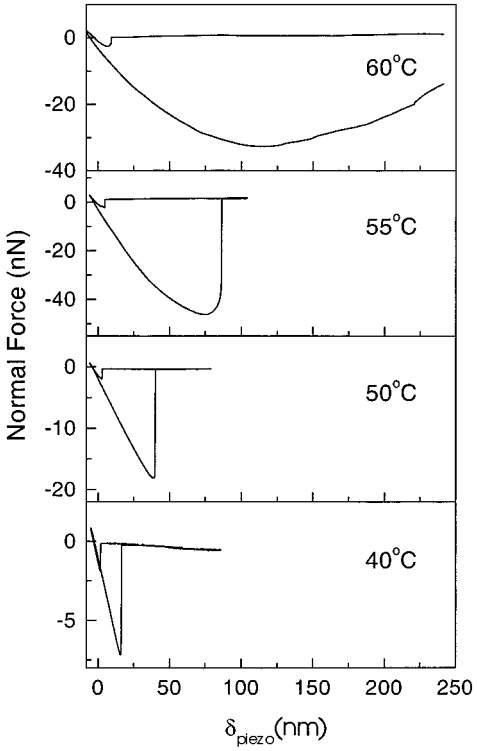

Figure 4. Series of force−distance curves obtained at the same probe rate, $f = 125$ Hz, but different temperatures: (top to bottom) $T = 60$, 55, 50, and 40 °C.

mechanical properties of the polymer, we gathered force−distance curves obtained at several representative temperatures as shown in Figure 4. At $T = 40$ °C, the slope of the curve remains unchanged during the entire pull-off process of the tip, and detachment between the tip and the sample is abrupt. This is in striking deviation from the data obtained at $T = 55$ and 60 °C, where substantial changes in the slope occurs before detachment. Such nonlinearity does not emanate from our setup as independent studies involving large bending of the cantilever show. Therefore, its origin must come from the sample. According to eq 1, slope of the force−distance curve, $dF/d\delta_{piezo}$, equals $k_c/(1 + k_c/k_s)$. We recall that $k_s = dF/d\delta$ is the effective force constant of the sample. A complete account of how the slope varies in a force−distance curve requires detailed analysis on the mechanics of the problem[26] and will not be discussed here. The basic idea is as follows: At low temperatures, $k_s \gg k_c$, and the slope $\sim k_c$ is independent of k_s. The

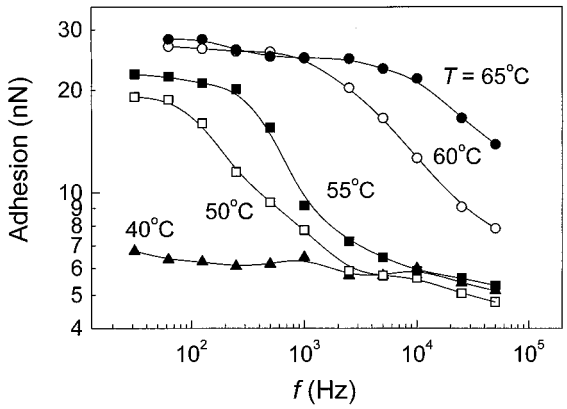

Figure 5. Adhesion vs f in log−log scales obtained at different temperatures from 40 to 65 °C as labeled. Solid lines are guides to the eye.

force−distance curves become sensitive to the mechanical properties of the sample, however, when $k_s \sim k_c$, which occurs when the polymer softens at elevated temperatures. At $T = 60$ °C, where F_{ad} starts to saturate, the force−distance curve shows a distinctive tail which extends by more than 120 nm beyond the minimum of the force−distance curve. On the basis of the foregoing discussion, k_s is comparable to or less than k_c in this case. Hence, the deformation suffered by the sample must be at least comparable with the amount of deflection undertaken by the tip. Such a large degree of elongation of the polymer is indicative of plastic deformation. Failure of the adhesive bond will most likely occur via cohesive fracture. The data presented so far demonstrate that adhesion is dependent on the mechanical strength of the polymer. To establish the correlation between adhesion and glass-to-rubber transition, we study the probe rate dependence of adhesion, with which equivalence between temperature and time can be investigated.

Probe Rate Dependence and the Master Curve. Figure 5 shows data for the probe rate dependence of adhesion in log−log scales obtained at various temperatures from 40 to 65 °C. The overall shape of these curves looks alike, except for an apparent shift of each curve with respect to one another along the abscissa: the higher the temperature, the farther the uprising of the adhesion data is shifted to the high-frequency side, reminiscent of the WLF scaling behavior. We rescale the abscissa for each curve by a temperature-dependent shift factor, $a_T^{AFM}(T)$, to produce a master curve using $T_{ref} = 55$ °C. The result is shown in the main panel of Figure 6, which carries clear similarity with the temperature dependence data of Figure 3, if an inversion of the abscissa were performed. The inset of the same figure shows the shift factors $a_T^{AFM}(T)$ that have been employed in producing the master curve in the main panel, together with the shift factor obtained for the bulk sample, $a_T^{bulk}(T)$, based on the data of Figure 1. Good agreement between the two indicates that the activation energy that governs the dynamical behavior at the glass-to-rubber transition is the same in the bulk and at the free surface of the polymer. To further establish the equivalence between time and temperature, several force−distance curves obtained at $T = 55$ °C but different probe rates are shown in Figure 7. As seen, with increasing f, the shape of the force−distance curves unfolds in a similar manner as with decreasing T shown in Figure 4, which indicates clearly that the

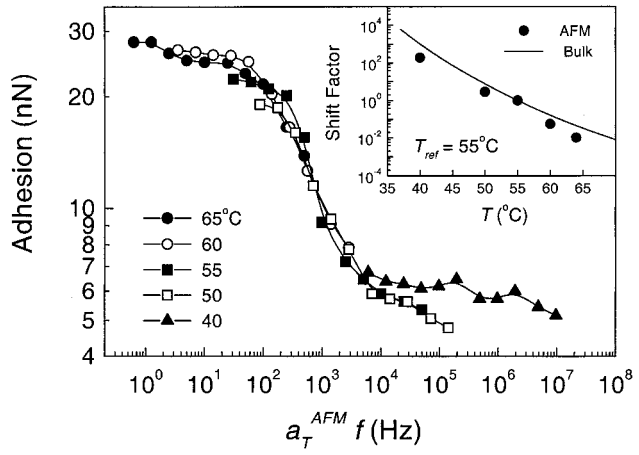

Figure 6. (main panel) Master curve of adhesion as a function of the rescaled frequency = $a_T^{AFM}f$ in a log−log plot, where a_T^{AFM} is the shift factor. Solid lines are guides to the eye. (inset) Shift factors, a_T^{AFM}, as a function of T (solid circles). The corresponding data that lead to the master curve of Figure 1, namely a_T^{bulk}, are also shown for comparison (solid line).

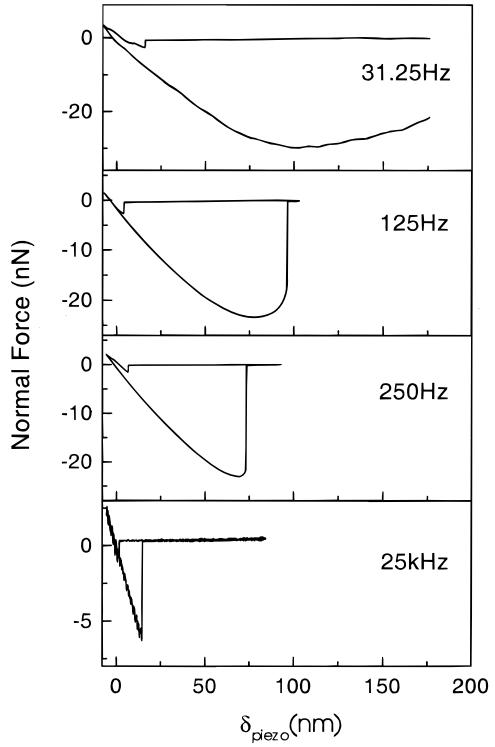

Figure 7. Series of force−distance curves obtained at the same temperature, T = 55 °C, but different probe rates: (top to bottom) f = 31.25 Hz ∼ a_T^{AFM}(60 °C) × 125 Hz, 125 Hz ∼ a_T^{AFM}(55 °C) × 125 Hz, 250 Hz ∼ a_T^{AFM}(53 °C) × 125 Hz, and 25 000 Hz ∼ a_T^{AFM}(40 °C) × 125 Hz. Close similarities with the respective data in Figure 4 are apparent, demonstrating the equivalence between time and temperature. The high-frequency noise notable in the data taken at f = 25 kHz comes from the AFM electronics.

present technique provides a direct probe for the viscoelastic properties of the polymer.

Discussion

In this section, an attempt will be made to explain the rise in F_{ad} with increasing T (or decreasing f) we have observed. As mentioned above, adhesion is independent of the loading history. According to the JKR theory, the contact configuration at any instant is as a result of an equilibrium balance between mechanical energy, elastic energy, and surface energy of the system. Hence, the present approach will be focused on the fracture mechanics at unloading. Calculations for the stress distribution, $\sigma(r)$, at the contact between an *elastic* sphere and a plane under the action of adherence had been outlined in ref 27. Tailored to our experimental conditions, it is (see Figure 3c)

$$\sigma(r) = \frac{2E}{\pi R(1-\nu^2)}\sqrt{(a^2 - r^2)} - \sqrt{\frac{2E\gamma a}{\pi(1-\nu^2)(a^2 - r^2)}} \quad (5)$$

where r is the distance measured from the center of the (circular) contact and the other symbols have the same meanings as were previously defined. Greenwood and Johnson[27] showed that this approach based on stress analysis was equivalent to the JKR model, for which the same results could be obtained by minimizing the integrated stress expressed in eq 5. As has been pointed out by these authors, the first term gives rise to a central compressive pressure and is responsible for producing the correct curvature for the deformation of the contacting bodies. The second term represents the tensile stress existing at the periphery of the contact. Irwin[28] showed that the Griffith criterion (i.e., the surface energy increment during the extension of a crack = the release of strain energy at the crack tip) would be satisfied if the tensile stress = $\lim_{r\to a} -\sqrt{[2E\gamma a/\pi(1-\nu^2)(a^2 - r^2)]}$, demonstrating the relevance of the second term in the growth of a crack. During pull-off at velocity V, there are thus two time scales: one, for the first term of eq 5, that characterizes the time over which the sample is deformed into the appropriate curvature, $\sim R/V$, and another one, for the second term of eq 5, that characterizes the growth of a crack tip, $\sim l/V$, with l being the crack length—the distance from the crack tip to a point where the tensile stress becomes negligible (see Figure 3c). We will now show that $l \ll R$ in our experiment. Since the strain energy exists only over a volume $\sim 2\pi^2 l^2 a$ about the crack tip,[28] the strain energy release per extension of the crack by length l is $\sim(\sigma_0^2/2E)(2\pi^2 l^2 a)$, where σ_0 is the strength of the adhesive bond, while the surface energy increment is $\sim 2\pi a l\gamma$. Using the Griffith criterion, we obtain $l \sim 2\gamma E/\pi\sigma_0^2$. Assuming that $\gamma \sim \sigma_0 z_0/2$ (where z_0 is the interatomic separation at the interface of the adhesive bond),[22,27] $z_0 \sim 0.3$ nm, γ = 24 erg cm^{-2}, and E = 0.6 GPa, we obtain $l \sim 0.36$ nm $\ll R$.

In the following, we will extend the above discussion to viscoelastic solids. The general paradigm involves replacing the elastic modulus, E (or the deformation $\propto 1/E$), in mathematical solutions to the corresponding elastic problem by the stress relaxation function, $E(t)$ (or the creep compliance function, $J(t) = 1/E(t)$).[27,29] If the time scale of the external force is short, i.e. $t \to 0$, E may be replaced by the instantaneous modulus, E_0. Similarly, if $t \to \infty$, the relaxed modulus, E_∞, may be used. According to Figure 1, with f being ∼31.25−50 000 Hz, the dynamic range of our AFM measurements falls in the intermediacy. Therefore, we may substitute $E(t)$ for E in the first term of eq 5. For the second term, however, the time scale is scaled down by a factor $\sim l/R$, which puts our experimental condition in the short-time limit for crack growth, and E_0 should therefore be used in place of E. We may now rewrite eq 5 for the present experiment:

$$\sigma(r) = \frac{2E(t)}{\pi R(1-\nu^2)}\sqrt{(a^2 - r^2)} - \sqrt{\frac{2E\gamma a}{\pi(1-\nu^2)(a^2 - r^2)}} \quad (6)$$

Clearly, eq 6 may be rearranged to the same form as eq 5 if we replace γ by an effective surface energy, $\gamma_{\text{eff}} = E_0\gamma/E(t) = \gamma J(t)/J_0$. As $F_{\text{ad}} \propto \gamma$ according to eq 3, this result indicates that the measured adhesive force should increase with t according to the creep compliance function, $J(t)$. We perform Fourier transform on the reciprocal of the complex modulus derived from the data of Figure 1. Upon normalization by the short time value, we obtain $J(t)/J(0)$, as shown in Figure 8 (solid line). For comparison, the normalized adhesion, $F_{\text{ad}}(t)/F_{\text{ad}}(0)$, is also displayed (dashed line) in the same figure. Good agreement between the two confirms the present interpretation. Deviations occurring at times >10 ms can be understood from the onset of mechanical yield in the polymer, evidenced from the appearance of a plastic deformation tail in the corresponding force−distance curves. Results based on this analysis indicate that no enhanced dynamical response can be found at the surface of the polymer. Previous studies by Kaijiyama et al.[11] using lateral force microscopy measurements on monodispersed PS (M_n = 4.9−140K Da) indicated that the polymer surface exhibited viscoelastic behavior even at T = 20 °C. According to studies on samples with different polydispersity,[11] the same authors concluded that the key to see the effect was to have low number-average molecular weight components with $M_n < \sim$30K Da. In the present experiment, commercial poly(*tert*-butyl acrylate) was used with $M_n \sim$ 8.5K Da and polydispersity, $M_w/M_n \sim 17$. Absence of an early onset of rubbery behavior in this experiment may be explained if the chain end group of our sample has much higher surface energy than that of the segment. Indeed, previous studies on thin films of similar acrylate polymers[30,31] showed no appreciable thickness dependence in T_g or dynamical properties of the polymer. It remains to study the surface viscoelastic properties of a system wherein a depression in T_g and hence enhanced molecular mobility was seen. It is noteworthy that increase in adhesion with T in the proximity of T_g was also observed in the AFM studies of Hammerschmidt et al.[13] on PS and PMMA. However, similar behavior was not found in PET by the same authors. It is possible that the interfacial energy between the polymer and the tip had been too weak, or the pull-off rate used was too fast, so that the feature had fallen outside the temperature range investigated. Nevertheless, results of this paper have demonstrated unambiguously that the current approach can be used to fully characterize the surface dynamical behavior of a polymer near the glass-to-rubber transition. Furthermore, based on the discussions given in the theory section, this technique will also provide a method to monitor any softening process that commences from the free surface. Presuming the conclusion that F_{ad} will be undermined unless the thickness of the softened layer is bigger than $R - \sqrt{(R^2 - a_{\text{detach}}^2)}$, so according to eq 4, one can in principle map out the entire proceeding by using AFM tips with different radii.

Conclusions

In conclusion, we have demonstrated that AFM adhesion measurements offer a powerful probe to examine the surface viscoelastic properties of a polymer, whence elaborate comparison was made against those of the bulk determined by conventional methods. Commercial polydispersed poly(*tert*-butyl acrylate) ($M_w \sim$ 148K Da, $M_w/M_n \sim 17$) has been used with bulk $T_g \sim$ 50 °C. Adhesion was generally determined as the pull-off force acted upon the cantilever at which detachment between the polymer and the cantilever tip occurs. At a small load of ~2.5 nN, we proposed theoretically that the present technique may monitor the growth of a hypothetical surface rubbery layer with increasing temperature as was described by Keddie et al. The adhesion was seen to increase with increasing temperature (from 30 to 65 °C) and decreasing probe rate (from 50 000 to 31.25 Hz.) The ultimate saturation at high temperatures and low probe rates was attributed to the occurrence of a mechanical yield in the polymer, in accordance with a long plastic deformation tail found in the respective force−distance curves. By rescaling the frequency axis of the adhesion data by the temperature-dependent shift factors, $a_T^{\text{AFM}}(T)$, a master curve, $F_{\text{ad}}(a_T^{\text{AFM}}(T)f)$, was obtained. Profound agreement between the shift factors thus obtained and those obtained based on shear modulus and torsion modulus measurements of the bulk sample indicates that the activation energy for the molecular relaxation of the polymer near the glass-to-rubber transition is the same in the bulk and at the free surface. Finally, adhesion as a function of reciprocal probe rate was compared with the creep compliance function, $J(t)$, of the bulk sample, whereby good agreement was also found. On the basis of a derivation using fracture mechanics of viscoelastic solids, we conclude that the molecular relaxation of our polymer sample at the free surface is not noticeably different than that of the bulk.

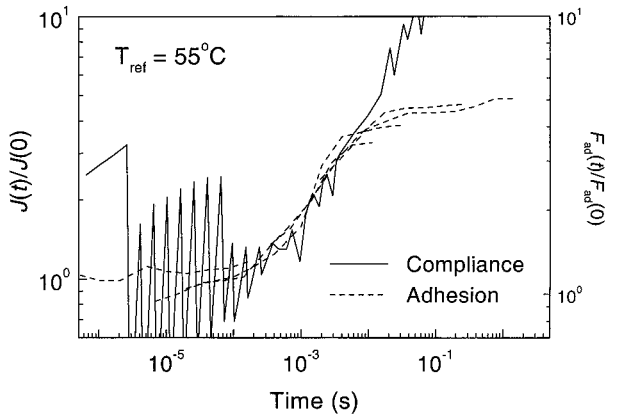

Figure 8. Comparison between the normalized creep compliance as a function of time in log−log scales (solid line) with the corresponding data for normalized adhesion (dashed line). The strong oscillations seen in the normalized creep compliance function is due to finite frequency cutoff in the Fourier transformation.

Acknowledgment. We are indebted to Prof. C. M. Chan and Ms. Pauline S. T. Leung (Chemical Engineering, HKUST) for assistance with the mechanical measurements of the bulk polymer and to Prof. Ben Zhong Tang's group (Chemistry, HKUST) for performance of the GPC measurements. General technical and instrumentation support by Materials Characterization and Preparation Facilities of HKUST is also gratefully acknowledged.

References and Notes

(1) Kittel, C. *Introduction to Solid State Physics*; John Wiley & Sons: New York, 1986.

(2) Jones, R. A. L.; Richards, R. W. *Polymers at Surfaces and Interfaces*; Cambridge University Press: Cambridge, 1999.
(3) Wu, X. Z.; Ocko, B. M.; Sirota, E. B.; Sinha, S. K.; Deutsch, M.; Cao, B. H.; Kim, M. W. *Science* **1993**, *261*, 1018.
(4) Theodorou, D. N. *Macromolecules* **1988**, *21*, 1391.
(5) Mayes, A. M. *Macromolecules* **1994**, *27*, 3114.
(6) Kaijiyama, T.; Tanaka, K.; Takahara, A. *Macromolecules* **1997**, *30*, 280.
(7) Zhao, W.; Zhao, X.; Rafailovich, M. H.; Sokolov, J.; Composto, R. J.; Smith, S. D.; Satkowski, M.; Russell, T. P.; Dozier, W. D.; Mansfield, T. *Macromolecules* **1993**, *26*, 561.
(8) Liu, Y.; Russell, T. P.; Samant, M. G.; Stohr, J.; Brown, H. R.; Cossy-Favre, A.; Diaz, J. *Macromolecules* **1997**, *30*, 7768.
(9) Xie, L.; DeMaggio, G. B.; Frieze, W. E.; DeVries, J.; Gidley, D. W.; Hristov, H. A.; Yee, A. F. *Phys. Rev. Lett.* **1996**, *74*, 4947.
(10) Tanaka, K.; Taura, A.; Ge, S.-R.; Takahara, A.; Kajiyama, T. *Macromolecules* **1996**, *29*, 3040.
(11) Tanaka, K.; Takahara, A.; Kaijiyama, T. *Macromolecules* **1997**, *30*, 6626.
(12) Kaijiyama, T.; Tanaka, K.; Takahara, A. *Macromolecules* **1995**, *28*, 3482.
(13) Hammerschmidt, J. A.; Gladfelter, W. L.; Haugstad, G. *Macromolecules* **1999**, *32*, 3360.
(14) Keddie, J. L.; Jones, R. A. L.; Cory, R. A. *Faraday Discuss.* **1994**, *98*, 219.
(15) Forrest, J. A.; Kalnoki-Veress, K.; Stevens, J. R.; Dutcher, J. R. *Phys. Rev. Lett.* **1996**, *77*, 2002.
(16) Blum, F. D.; Xu, G.; Liang, M.; Wade, C. *Macromolecules* **1996**, *29*, 8740.
(17) Park, J.-Y.; McKenna, B., to be published in *Phys. Rev. B*.
(18) Tsui, O. K. C.; Russell, T. P.; Hawker, C. J., preprint 98.
(19) See for example: Wallace, W. E.; van Zanten, J. H.; Wu, W. L. *Phys. Rev. E* **1995**, *52*, 3329. van Zanten, J. H.; Wallace, W. E.; Wu, Wen-li *Phys. Rev. E* **1996**, *53*, 2053. It should also be remarked that the T_g of the P*t*BuA film used in this study has been found to be 45 °C using ellipsometry. Comparing with the value of 50 °C obtained by DSC, no effect on the T_g of the thin film coming from an attractive interaction at the polymer/substrate interface, if any, is evident at this thickness.
(20) Kaelble, D. H. *J. Adhes.* **1969**, *1*, 102.
(21) Gent, A. N.; Petrich, R. P. *Proc. R. Soc. London, A* **1969**, *310*, 433.
(22) Wu, S. *Polymer Interface and Adhesion*; Marcel Dekker: New York, 1982.
(23) Williams, M. L.; Landel, R. F.; Ferry, J. D. *J. Am. Chem. Soc.* **1955**, *77*, 3701.
(24) Johnson, K. L.; Kendall, K.; Roberts, A. D. *Proc. R. Soc. London, A* **1971**, *324*, 301.
(25) Ogletree; D. F.; Carpick; R. W.; Salmeron; M. *Rev. Sci. Instrum.* **1996**, *67*, 3298.
(26) Tsui, O. K. C., unpublished results.
(27) Greenwood, J. A.; Johnson, K. L. *Philos. Mag. A* **1981**, *43*, 697.
(28) Irwin, G. R. *J. Appl. Mech.* **1957**, *24*, 361.
(29) Ting, T. C. T. *J. Appl. Mech.* **1966**, *33*, 845.
(30) Hall, D. B.; Miller, R. D.; Torkelson, J. M. *J. Polym. Sci., Part B: Polym. Phys.* **1997**, *35*, 2795.
(31) Dhinojwala, A.; Wong, G. K.; Torkelson, J. M. *Macromolecules* **1993**, *26*, 5943.

MA991473X